

# Molecular Recognition of the Human Coactivator CBP by the HIV-1 Transcriptional Activator Tat<sup>†</sup>

Andrew C. Vendel<sup>‡</sup> and Kevin J. Lumb<sup>\*,‡,§</sup>

Department of Biochemistry and Molecular Biology, Department of Chemistry,  
Colorado State University, Fort Collins, Colorado 80523-1870

Received October 14, 2002; Revised Manuscript Received November 25, 2002

**ABSTRACT:** HIV-1 Tat is required for the expression of the viral genome. Tat binds to an RNA stem-loop and mediates the recruitment of human coactivators to facilitate HIV-1 transcription. The coactivator and acetyltransferase CREB binding protein (CBP), and the paralog p300, are recruited to the HIV-1 promoter by Tat. Here we identify the interacting domains of Tat and CBP. Circular dichroism and pulldown assays show that full-length Tat binds to the KIX domain of CBP, but not to the C/H1 or CR2 domains. Circular dichroism and NMR studies of Tat deletion mutants localize the KIX-binding domain of Tat to the N-terminal 24 residues of Tat. Transient cotransfections demonstrate that exogenous KIX behaves as a dominant negative to Tat-mediated transcription in human T-cells, suggesting that Tat and KIX interact *in vivo*. These findings indicate that Tat targets the KIX domain of CBP and provide insight into the molecular interactions involved in regulating HIV-1 gene expression.

Expression of the HIV-1<sup>1</sup> genome requires both human and viral transcription factors (1, 2). The HIV-1 LTR promoter is reminiscent of human protein-coding promoters, and viral expression employs the human general transcription machinery, including RNA polymerase II, general transcription factors, coactivators, and the activators NF- $\kappa$ B and SP1 (1, 2). In addition to the host proteins, the HIV-1 transactivator Tat is needed for viral RNA synthesis and propagation (1, 2). Attenuated viruses with mutated Tat integrate the HIV-1 genome into human cells, but are unable to propagate (3, 4). Unlike human transcriptional activators, which bind DNA, Tat binds RNA at the stem loop of TAR through a basic arginine rich motif (ARM, residues 49–57 of Tat) (1, 2). Once bound to TAR, Tat recruits the endogenous cellular factors involved in elongation such as P-TEFb, which hyperphosphorylates the C-terminal domain of the large subunit of RNA polymerase II (5).

The human genome is packaged into nucleosomes that repress transcription until remodeled following histone acetylation (6). Since the incorporated HIV-1 genome is also packaged into nucleosomes, recruitment of proteins that regulate the modification of the nucleosomal architecture downstream of the HIV-1 start site is likely to be needed for viral gene expression and replication. For example, nucleosome 1 near the transcription start site of the 5' LTR is disrupted during transcriptional activation (7, 8), and acetylation of the histone tails of nucleosome 1 is coupled with transcriptional activation in a Tat dependent manner (9). It is likely that Tat, in part, recruits proteins involved in nucleosome remodeling, including acetyltransferases, to facilitate viral gene expression (9–11).

CBP is a large protein of 2441 amino acids comprised of several autonomously functional domains that contribute to different facets of CBP function (Figure 1) (12, 13). CBP interacts with numerous mammalian and viral transcription activators, coactivators, corepressors and the general transcription machinery (12, 13). For example, the C/H1 domain binds NF- $\kappa$ B, HIF-1, and HPV E6, the CR2 domain binds p53, SRC-1, and HTLV-1 Tax, and the KIX domain binds many cellular and viral transcriptional activators including CREB, HTLV-1 Tax, MLL, and c-Jun (12, 13). The combination of acetyltransferase activity and ability to interact with multiple transcription factors endows upon CBP a widespread role in transcription during basic cellular process such as cell growth, differentiation and tumor suppression (12, 13).

Tat interacts with the histone acetyltransferase CBP and with the highly related protein p300 (10, 11). Recruitment of CBP by Tat during HIV-1 gene expression may provide a mechanism for nucleosome remodeling and transcription regulation (10, 11). Beyond the protein–protein interactions

<sup>†</sup> Supported by the American Cancer Society (RSG-02-051-GMC).

<sup>\*</sup> To whom correspondence should be addressed. E-mail: lumb@lamar.colostate.edu.

<sup>‡</sup> Department of Biochemistry and Molecular Biology.

<sup>§</sup> Department of Chemistry.

<sup>1</sup> Abbreviations: 1D, one-dimensional;  $[\theta]_{222}$ , molar ellipticity at 222 nm; AIDS, acquired immune deficiency syndrome; C/H1, Cys/Hist-rich region 1 of CBP; CBP, CREB-binding protein; CD, circular dichroism; CR2, conserved region 2 of CBP; CREB, CRE-response element binding protein; DSS, sodium 2,2-dimethyl-2-silapentane-5-sulfonate; DTT, dithiothreitol; EDTA, ethylenediamine tetraacetic acid; GST, glutathione-S-transferase; HIF-1, hypoxia inducible factor-1; HIV-1, human immunodeficiency virus type 1; HPLC, high-performance liquid chromatography; HTLV-1, human T cell leukemia virus type 1; IPTG, isopropyl- $\beta$ -D-thiogalactoside; KID, kinase inducible domain of CREB;  $K_d$ , dissociation constant; KIX, KID-interacting domain of CBP; LTR, long terminal repeat; NMR, nuclear magnetic resonance; P/CAF, p300 and CBP associated factor; ppm, parts per million; TAR, transactivation region; Tat, transactivator of transcription; TFA, trifluoroacetic acid; TOCSY, total correlation spectroscopy.

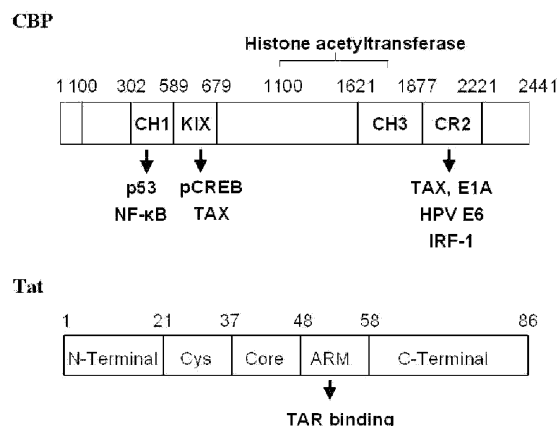


FIGURE 1: Schematic representation of the domain structures of CBP and Tat. CBP possesses multiple, functionally independent, protein-interacting domains, including C/H1 (residues 300–450), KIX (residues 589–679), and CR2 (residues 2055–2150) (12, 13). Some transcriptional activators that bind C/H1, KIX, and CR2 are listed. Tat comprises the N-terminal domain, Cys-rich domain, core domain, and ARM (1).

involved in viral transcription, Tat also makes contacts with a number of cellular transcription factors, coactivators, and other cellular proteins that may disrupt normal cellular function and contribute to infection-associated pathogenesis (14–16). For example, the C-terminus of a 101-amino acid version of Tat, which is deleted in the 86-residue Tat, globally represses the histone acetyltransferase activity of CBP and other HAT proteins and decreases the expression of a number of cellular, but not viral, genes (14–16).

Although CBP plays an essential role in Tat-dependent HIV-1 transcription (10, 11), the molecular basis of CBP recruitment by Tat during viral gene expression is unclear. Here we show that the N-terminus of Tat recognizes the KIX domain of CBP *in vitro* and that the interaction modifies Tat behavior *in vivo*. Our results implicate KIX as the domain of CBP that is targeted by Tat during HIV-1 propagation.

## EXPERIMENTAL PROCEDURES

**Protein Preparation and Purification.** The Tat used here corresponds to the 86-residue Tat from the HIV-1 isolate HXB2. The amino acid sequence, derived by DNA sequencing of the expression plasmid, is

GSH MEPVDPRLEP WKHPGSQPKT ACTNCYCKKC  
CFHCQVCFIT KALGISYGRK KRRQRRRPPQ  
GSQTHQVSLK KQPTSQSRGD PTGPKE

The N-terminal residues GSH are derived from the pET-15b expression plasmid.

Tat was expressed as an N-terminal His-tagged fusion protein with a pET-15b plasmid (pET-15b:Tat) harboring a PCR product encoding Tat amplified from the plasmid GST-Tat (86R) obtained from the NIH AIDS Research and Reference Reagent Program (17). The coding sequence for Tat was confirmed with dRhodamine sequencing. Tat was expressed in *Escherichia coli* strain Rosetta BL21 (DE3) pLysS (Novagen). Cells were grown at 37 °C to an optical density at 600 nm of 0.8 and induced with 0.5 mM IPTG for 2 h. Tat was purified from the insoluble cell-lysate fraction resuspended in 6 M urea, 20 mM Tris-base, 500

mM NaCl, and 50 mM imidazole, pH 7.8, with His-bind resin (Novagen). Tat was eluted with 20 mM Tris-base, 500 mM NaCl, and 400 mM imidazole, pH 7.8. The His-tag was then cleaved with thrombin (Novagen) in elute buffer, pH 8.4, overnight at room temperature. Tat was treated with 50 mM EDTA and 0.1 M DTT, pH 8.4, prior to final purification with reversed-phase C<sub>18</sub> HPLC using a linear water/acetonitrile gradient containing 0.1% TFA. The identity of Tat was confirmed with electrospray mass spectrometry, and the observed and expected masses agreed to within 1 Da.

The C-terminal, RNA-binding domain of HIV-1 Tat (ARM) was expressed as an N-terminal His-tagged fusion protein from a pET-15b plasmid (pET-15b:ARM) harboring a PCR product encoding residues 48–86 of Tat amplified from pET-15b:Tat. The coding sequence of ARM was confirmed with dRhodamine sequencing. ARM was expressed in *E. coli* strain Rosetta BL21 (DE3) pLysS (Novagen). Cells were grown at 37 °C to an optical density at 600 nm of 0.8 and induced with 0.5 mM IPTG for 2 h. ARM was purified from the insoluble cell-lysate fraction resuspended in 6 M urea, 20 mM Tris-base, 500 mM NaCl, and 50 mM imidazole, pH 7.8, with His-bind resin (Novagen). ARM was eluted with 20 mM Tris-base, 500 mM NaCl, and 400 mM imidazole, pH 7.8. The His-tag was cleaved with thrombin (Novagen) in elute buffer, pH 8.4, overnight at room temperature. ARM was treated with 50 mM EDTA and 0.1 M DTT, pH 8.4, prior to final purification with reversed-phase C<sub>18</sub> HPLC using a linear water/acetonitrile gradient containing 0.1% TFA. The identity of ARM was confirmed with electrospray mass spectrometry, and the observed and expected masses agreed to within 1 Da.

Tat<sub>1–24</sub>, corresponding to residues 1–24 of Tat from HIV-1 isolate HXB2, was synthesized on MBHA (4-methylbenzhydrylamine hydrochloride salt) resin (100–200 mesh) using manual Boc chemistry (18). The side chains of Arg, Asp, Cys, Gln, Glu, His, Lys, Ser, Thr, and Trp were protected during Boc chemistry with Tos, Bzl, MeBzl, Xan, Bzl, DNP, ClZ, Bzl, Bzl, and CHO, respectively. Tat<sub>1–24</sub> was purified by reversed-phase C<sub>18</sub> HPLC using a linear water/acetonitrile gradient containing 0.1% TFA. The identity of Tat<sub>1–24</sub> was confirmed with electrospray mass spectrometry, and the observed and expected masses agreed to within 1 Da.

KIX (residues 589–679 of human CBP with an additional N-terminal Met) was expressed in *E. coli* strain BL21 (DE3) pLysS and purified as described previously (19, 20). Final purification was by reversed-phase C<sub>18</sub> HPLC using a linear water/acetonitrile gradient containing 0.1% TFA. The identity of KIX was confirmed with electrospray mass spectrometry, and the observed and expected masses agreed to within 1 Da.

C/H1 (residues 300–450 of murine CBP) was expressed as a GST-fusion protein in *E. coli* strain BL21 (DE3) pLysS using the plasmid pGST-C/H1 (21). Cells were grown at 37 °C to an optical density at 600 nm of 0.8 and induced with 1 mM IPTG for 3 h. GST-C/H1 was purified from the soluble cell-lysate fraction with glutathione sepharose 4B (AP Biotech). GST-C/H1 was eluted with 20 mM Tris-base, 150 mM NaCl, and 5 mM glutathione, pH 7.8. The GST-tag was cleaved in elute buffer with thrombin (Novagen) at 25 °C overnight. Cleaved protein was dialyzed into GST-binding

buffer and C/H1 was separated from GST by further GST-affinity chromatography. Final purification was by reversed-phase C<sub>18</sub> HPLC. The identity of C/H1 was confirmed with electrospray mass spectrometry, and the observed and expected masses agreed to within 1 Da.

HPLC-purified CR2 (conserved region 2, residues 2055–2150 of murine CBP) was a generous gift of S. J. McBryant.

All HPLC-purified proteins were stored as a lyophilized powder and dialyzed against 10 mM sodium phosphate, 150 mM NaCl, and 1 mM DTT, pH 7.0, overnight before use.

GST-fusion proteins of HIV-1 isolate HBX2 Tat (expressed with GST-Tat 1 86R, NIH AIDS Research & Reference Reagent Program) (17), C/H1 (residues 300–450 of murine CBP, expressed with plasmid pGST-C/H1, gift of J. K. Nyborg) (21), KIX (residues 451–720 of murine CBP, expressed with plasmid pGST-KIX, gift of J. K. Nyborg) (22), and CR2 (residues 2055–2150 of murine CBP, expressed with plasmid pGST-CR<sub>2055–2150</sub>, gift of J. K. Nyborg) (23) were expressed in *E. coli* strain BL21 (DE3) pLysS. Cells were grown to an optical density at 600 nm of 0.8 at 37 °C and induced with 1 mM IPTG for 3 h. GST-fusion proteins were purified from the soluble fractions by cation-exchange chromatography on HiTrap SP (AP Biotech) followed by GST-affinity chromatography with glutathione sepharose 4B (AP Biotech). Proteins were dialyzed in 10 mM sodium phosphate, 150 mM NaCl, and 10% glycerol, pH 7.0 and stored at –70 °C.

**Pulldown Binding Assays.** GST-fusion proteins (25 pmol) were bound to a 30  $\mu$ L slurry of glutathione sepharose 4B (AP Biotech) in 200  $\mu$ L of GST binding buffer (50 mM Tris-base, 150 mM NaCl, 100 mM NaF, 200  $\mu$ M sodium orthovanadate, 0.5% NP-40, and 10 mM DTT, pH 8.0) for 2 h at 4 °C. Bound GST-fusion proteins were incubated in 200  $\mu$ L of binding buffer with 25 pmol of target protein for 2 h at 4 °C. Bound proteins were washed four times with wash buffer (50 mM Tris-base, 350 mM NaCl, 100 mM NaF, 200  $\mu$ M sodium orthovanadate, 0.5% NP-40, and 10 mM DTT, pH 8.0) and eluted by boiling in SDS–PAGE load buffer (50 mM Tris-base, 0.06% bromophenol blue, 2% SDS, 10% glycerol, and 1 mM 2-mercaptoethanol). Target proteins were resolved with 16% SDS–PAGE. Proteins were blotted onto nitrocellulose (Bio-Rad). KIX was detected with SYPRO ruby blot stain (Bio-Rad) per the manufacturer's protocol. Tat was detected with a Tat specific rabbit antibody (HIV-1 BH10 Tat antiserum) obtained from the NIH AIDS Research and Reagent Reference Program (24, 25) visualized by chemiluminescence (ECL Plus, AP Biotech) with a Molecular Dynamics STORM 860 fluorescence imaging instrument.

**Protein Concentration Determination.** Concentrations of protein stock solutions used to prepare CD and NMR samples were determined by absorbance in 6 M GuHCl, 10 mM sodium phosphate, and 150 mM sodium chloride, pH 6.5 at 25 °C (26). Extinction coefficients for Tat, KIX, C/H1, and Tat<sub>1–24</sub> at 280 nm of 8730, 12 090, 6170, and 5690 M<sup>–1</sup> cm<sup>–1</sup> were used, respectively. Extinction coefficients for ARM and CR2 at 276 of 1450 and 6970 M<sup>–1</sup> cm<sup>–1</sup> were used, respectively.

**CD Spectroscopy.** CD spectra were acquired with a Jasco J720 spectrometer. Samples were prepared in 10 mM sodium phosphate and 50 mM sodium chloride, pH 7.0, and contained 10  $\mu$ M of each protein. Spectra comprised 25 scans

recorded at 10 °C. The normalized molar ellipticity  $[\theta]$  was calculated from the measured ellipticity  $\theta$  using  $[\theta] = \theta \times 100/(nlc)$ , where  $n$  is the total number of residues of the protein or mix of proteins,  $c$  is the total protein concentration in mM, and  $l$  is the path length in centimeters. Binding was detected by differences in observed spectra of the protein mixes from the spectra expected if the two proteins do not interact, calculated as the normalized sum of the spectra of the individual proteins. Two proteins do not bind if the observed and calculated spectra overlap. Two proteins do bind if the observed and calculated spectra do not overlap, which presumably reflects a change in the secondary structure upon complex formation.

**NMR Spectroscopy.** <sup>1</sup>H NMR spectra were acquired with a Varian Unity Inova operating at 500.1 MHz for <sup>1</sup>H and referenced to internal DSS at zero ppm. Samples were prepared in 10 mM sodium phosphate and 50 mM NaCl, pH 7.0, lyophilized, and resuspended in D<sub>2</sub>O. pH was adjusted to 7.0, uncorrected for the isotope effect.

The  $K_d$  for the Tat<sub>1–24</sub>–KIX complex was determined at 10 °C from changes of the His 13 C<sub>2</sub>H chemical shift as 50  $\mu$ M Tat<sub>1–24</sub> was titrated with 0–150  $\mu$ M KIX. Chemical shifts were measured from 1D spectra collected with a digital resolution of approximately 0.001 ppm/point. The  $K_d$  was obtained from changes in the <sup>1</sup>H chemical shift with KIX concentration using

$$\delta = \delta_f + \delta_b - \delta_f(P + L + K_d) - \{(P + L + K_d)^2 - (4PL)\}^{0.5}/2[P]$$

where  $\delta$  is the chemical shift at KIX concentration  $L$ ,  $\delta_f$  and  $\delta_b$  are the free and bound chemical shifts, respectively, and  $P$  is the concentration of Tat<sub>1–24</sub>. The fit assumes a 1:1 stoichiometry. The resonances of the two aromatic side chains of Tat (Trp 11 and His 13) were assigned at 10 °C from a TOCSY spectrum collected with a 60 ms DIPSI sequence. The sample contained 0.5 mM Tat<sub>1–24</sub> in 10 mM sodium phosphate and 50 mM NaCl, pH 7.0.

**Transient Cotransfection Assay.** Mammalian expression plasmids encoding HIV-1 Tat (pSV2Tat72) and an LTR promoter linked to a luciferase reporter gene (pBlue3'LTR-luc-A) were obtained from the NIH AIDS Research and Reference Reagent Program (27). Mammalian expression plasmids for KIX (pRSV–KIX, encoding residues 459–679 of murine CBP) and CR2 (pCMV–CR2, encoding residues 2003–2212 of murine CBP) were gifts of J. K. Nyborg (22, 23). Jurkat cells grown in Iscove's modified Delbecco's media (IMDM) supplemented with 10% fetal bovine serum, 2 mM L-glutamine, and penicillin-streptomycin were transfected with plasmids using lipofectamine (Invitrogen). The total DNA for each transfection was normalized to 2  $\mu$ g with pUC-19. Cells were lysed 24 h posttransfection, and LTR luciferase activity was normalized against 10 ng/transfection pRL-TK Renilla luciferase (Promega). Luciferase activity was monitored with a Turner Designs model TD 20-e luminometer. Tat expression was confirmed with Western blot analysis of the whole-cell lysate using a Tat specific rabbit antibody (HIV-1 BH10 Tat antiserum) (25) obtained from the NIH AIDS Research and Reagent Reference Program visualized by chemiluminescence (ECL Plus, AP Biotech) with a Molecular Dynamics STORM 860 fluorescence imaging instrument.



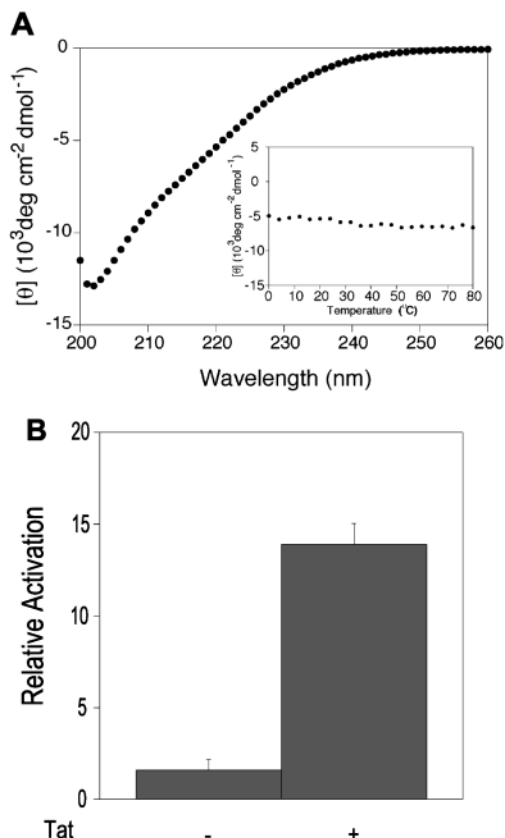


FIGURE 2: (A) CD spectroscopy indicates that full-length Tat is largely unfolded in isolation. Tat is devoid of signature CD signals that reflect significant helix or sheet formation, and has a minimum at 202 nm that is indicative of an unfolded protein. The CD signal at 222 nm becomes slightly more negative with increasing temperature (insert), which is the opposite behavior expected for a typical globular protein. (B) Tat is functional for cellular uptake and nuclear import. Recombinant Tat added to transfected human T cells activates luciferase expression from the HIV-1 LTR promoter above basal levels. Collectively, these results show that the Tat used here is an intrinsically disordered, biologically active protein.

**Tat Functional Assay.** Purified, recombinant Tat was tested for biological activity on the basis of cellular uptake (27) by Jurkat cells transfected with the LTR-luciferase reporter plasmid (pBlue3'LTR-luc-A) obtained from the NIH AIDS Research and Reference Reagent Program (28, 29). Jurkat cells were transfected as described above with 400 ng of pBlue3'LTR-luc-A plasmid and 10 ng of pRL-TK Renilla luciferase plasmid (Promega) using lipofectamine (Invitrogen). The total DNA for each transfection was normalized to 2  $\mu\text{g}$  with pUC-19. Cells were grown in the presence or absence of 3.33  $\mu\text{M}$  Tat protein. Cells were lysed 24 h posttransfection, and LTR luciferase activity was normalized against 10 ng/transfection pRL-TK Renilla luciferase (Promega). Luciferase activity was monitored with a Turner Designs model TD 20-e luminometer.

## RESULTS

**Intrinsic Structural Disorder of Tat.** The CD spectrum of Tat is reminiscent of an unfolded protein, with a minimum at 202 nm and a lack of spectral characteristics above 210 nm indicative of helix or sheet formation (Figure 2A). The CD signal at 222 nm becomes slightly more negative with increasing temperature (Figure 2A), which is the opposite behavior expected for a typical globular protein.

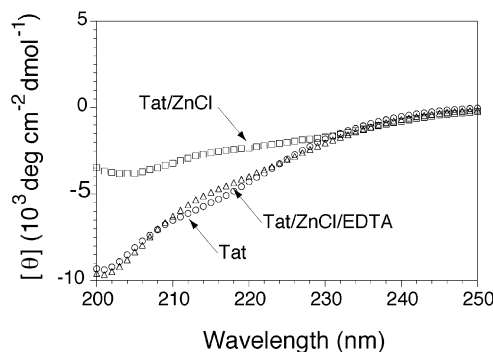


FIGURE 3: CD spectroscopy shows that Tat (○) undergoes a minor conformational change upon addition of 1 mM ZnCl<sub>2</sub> (□). This change is reversible with the addition of 1 mM EDTA (△). The observable changes in the CD signal are not indicative of a zinc-induced, global folding transition.

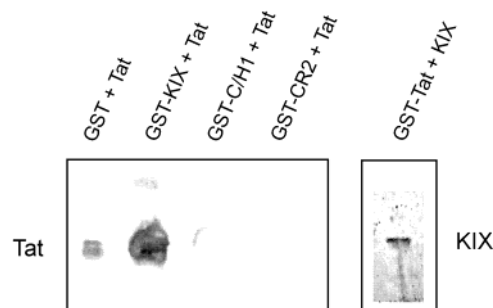


FIGURE 4: GST-pulldown screening of CBP domains for Tat binding. Tat interacts with GST-KIX, but not with GST, GST-C/H1, or GST-CR2. Tat was detected by Western blotting with a Tat-specific antibody. A reciprocal experiment shows that GST-Tat binds KIX.

A functional property of Tat is cellular uptake and nuclear import (27). This feature is maintained by the Tat used here (Figure 2B), demonstrating that the Tat is biologically active by its ability to activate transcription from the LTR promoter.

The Cys-rich domain (Figure 1) of Tat may bind  $\text{Zn}^{2+}$  (30, 31). Addition of  $\text{Zn}^{2+}$  causes some changes in the CD spectrum, including a reduced intensity of the unfolded signature band at 202 nm (Figure 3). However, the changes are not indicative of a large-scale folding transition upon binding  $\text{Zn}^{2+}$ , as seen for bona fide Zn-binding proteins (32).

These results indicate that Tat is biologically active and largely unfolded at neutral pH both in the presence and absence of  $\text{Zn}^{2+}$ , although the results do not preclude the local formation of short elements of secondary structure. This result is in accord with a previous NMR study of the 86 amino acid Tat from the HIV-1 Zaire 2 isolate (33).

**Tat Associates with KIX in Vitro.** Two different in vitro binding assays were used to screen for the binding of Tat to discrete CBP domains. Pull-down assays were used initially to screen GST-tagged C/H1, CR2, and KIX domains of CBP for Tat binding. In this assay format, Tat binds to the GST-KIX fusion protein, but not to GST, GST-C/H1, or GST-CR2 (Figure 4). In a reciprocal experiment, GST-Tat binds untagged KIX (Figure 4). These results suggest that Tat binds to KIX and not to C/H1 or CR2.

CD spectroscopy was then used to test domains of CBP for direct Tat binding. The CD spectrum of free KIX is indicative of a helical protein (Figure 5A), in accord with the NMR structure of KIX (34) and previous CD results (19). Addition of Tat results in a significant increase in ellipticity

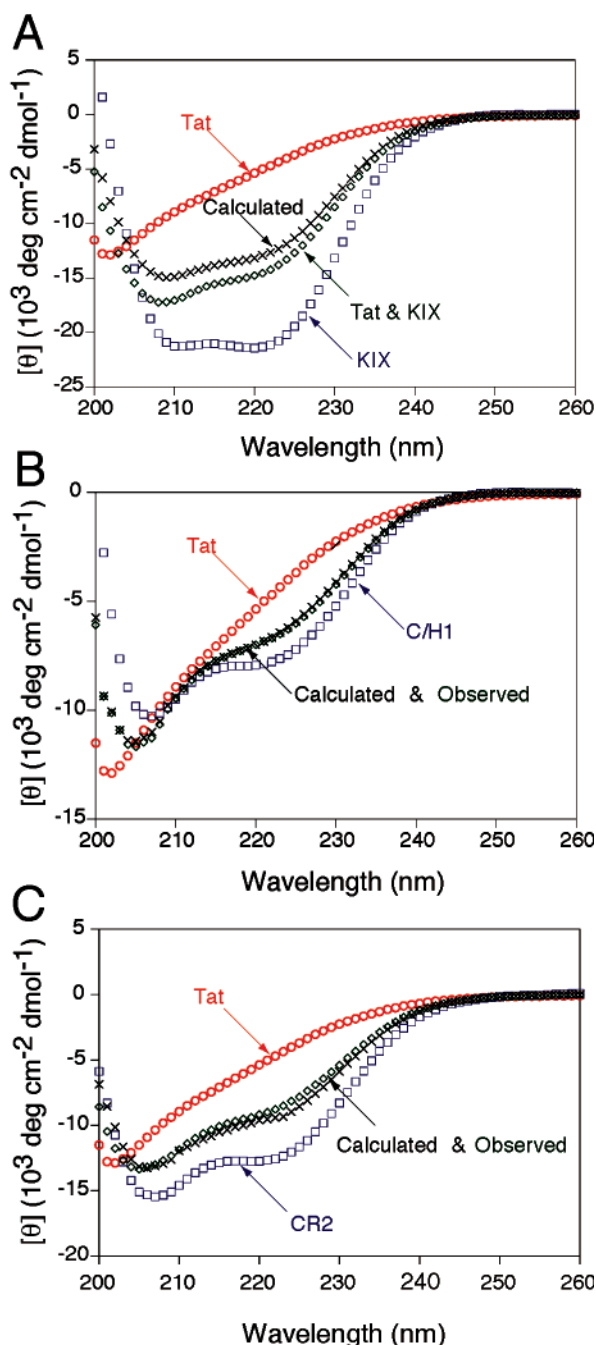


**FIGURE 5:** CD screening CBP domains for Tat binding. Tat binds KIX, but not C/H1 or CR2. (A) Mixing of Tat (○) with KIX (□) results in a spectrum (◇) with greater helicity at 208 and 222 nm than expected from the sum of the spectra of the two isolated proteins (×), suggesting that KIX forms a complex with Tat in solution. (B) Mixing Tat (○) and C/H1 (□) results in a spectrum (◇) that is equal to the sum of the spectra of the two isolated proteins (×), suggesting that Tat and C/H1 do not interact. (C) Mixing Tat (○) and CR2 (□) results in a spectrum (◇) that is equal to the sum of the spectra of the two isolated proteins (×), suggesting that Tat and CR2 do not interact. Reproducible results were obtained from three independent experiments. On the basis of variations in CD spectra collected with independently prepared, ostensibly identical samples, the error in  $[\theta]_{222}$  is less than 4%. The difference between the calculated and observed spectra of the Tat-KIX complex is 11% of the calculated spectrum.

over the calculated spectrum of noninteracting Tat and KIX (Figure 5A). This result suggests that Tat binds the KIX domain of CBP. In addition, the CD data suggest that complex formation is coupled with an increase in secondary

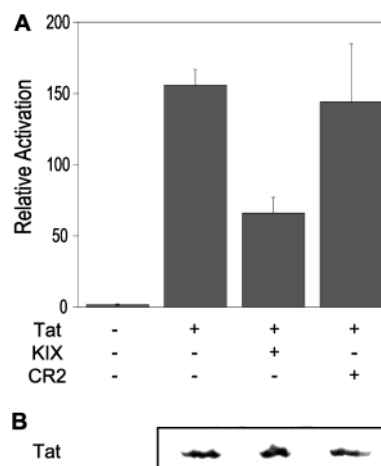


**FIGURE 6:** KIX and Tat interact in human T cells. (A) The relative fold activation of luciferase expression under the control of the HIV-1 LTR promoter was monitored to the extent of Tat activation. Plasmids encoding Tat and an LTR-luciferase reporter were cotransfected with plasmids encoding either KIX or CR2. KIX squelches Tat-dependent luciferase expression, suggesting that KIX acts as a dominant-negative for Tat mediated transcription in vivo. The effect is specific for KIX, since CR2 does not affect Tat-dependent expression. The finding that Tat interacts with KIX, but not CR2, in T cells is in accord with the in vitro binding assays. (B) Western blot analysis with Tat antiserum of whole-cell lysates suggests that the levels of Tat protein are unaffected by coexpression with KIX or CR2.

structure (folding). The association of Tat and KIX was also monitored with CD spectroscopy in the presence of  $\text{Zn}^{2+}$ , and very similar results to those shown in Figure 5A were obtained (data not shown).

The CD spectrum of C/H1 is reminiscent of a partially helical protein (Figure 5B), in accord with previous results (35). Addition of Tat to C/H1 results in a CD spectrum that is essentially identical to the calculated spectra of noninteracting C/H1 and Tat (Figure 5B), suggesting that Tat does not bind the C/H1 domain. The CD spectrum of CR2 is reminiscent of a partially helical protein (Figure 5C). Addition of Tat to CR2 results in a CD spectrum that is essentially identical to the calculated spectra of noninteracting C/H1 and Tat (Figure 5C), suggesting that Tat does not bind the CR2 domain (Figure 5C).

Collectively, these results suggest that Tat binds the KIX domain of CBP, and that binding is accompanied by secondary structure formation.

**KIX Mediates Tat-Activated Transcription in Human T Cells.** Since KIX interacts with Tat in vitro, KIX is expected to act as a dominant negative regulator of Tat activation in vivo. Therefore, Tat-dependent transcription in human T cells was analyzed in the presence and absence of KIX and CR2. T cells (Jurkat) were transiently cotransfected with a luciferase reporter gene fused to the HIV-1 LTR promoter with plasmids encoding Tat, KIX, or CR2. Tat efficiently activates transcription from the HIV-1 promoter, as expected (Figure 6A). KIX expression squelches Tat-mediated transcription, suggesting that KIX can act as a dominant negative to CBP and disrupt normal Tat function. CR2, which does not bind Tat in vitro (Figure 5C), does not suppress Tat-mediated transcription in T cells, showing that the squelching was specific to KIX. Western blot analysis suggests that Tat expression is not reduced by coexpression with KIX or CR2 (Figure 6B), suggesting that the observed changes in Tat-

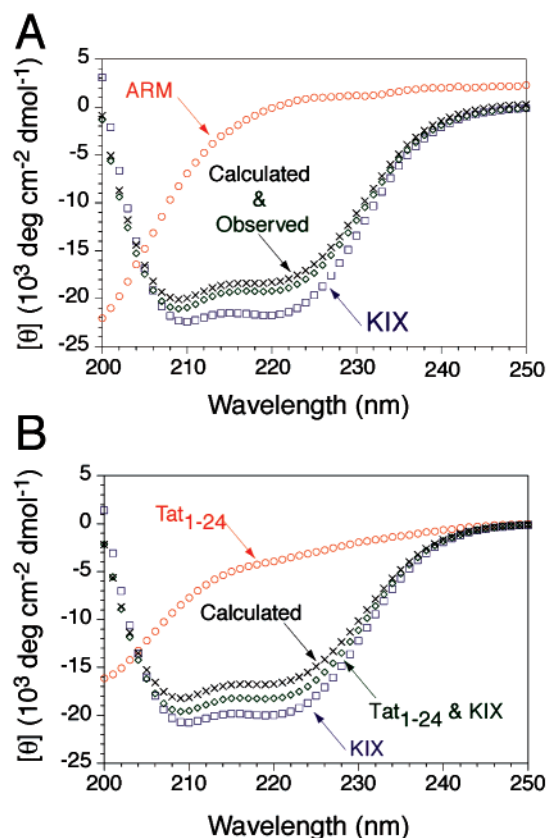


FIGURE 7: Association of KIX and the N-terminus of Tat monitored with CD spectroscopy. (A) Mixing of ARM ( $\circ$ ) with KIX ( $\square$ ) results in a spectrum ( $\diamond$ ) that is very similar to the sum of the spectra of the two isolated proteins ( $\times$ ), suggesting that the C-terminus of Tat and KIX do not interact. (B) Mixing Tat<sub>1–24</sub> ( $\circ$ ) with KIX ( $\square$ ) results in a spectrum ( $\diamond$ ) with greater helicity at 208 and 222 nm than expected from the sum of the spectra of the two isolated proteins ( $\times$ ), suggesting that Tat<sub>1–24</sub> binds with KIX. Reproducible results were obtained from two independent experiments. On the basis of variations in CD spectra collected with independently prepared, ostensibly identical samples, the error in  $[\theta]_{222}$  is approximately 3%. The difference between the calculated and observed spectra of the Tat<sub>1–24</sub>–KIX complex is 9% of the calculated spectrum.

mediated transcription do not reflect changes in the level of Tat protein. These *in vivo* functional results corroborate the *in vitro* finding that the KIX domain of CBP binds Tat.

**The N-Terminus of Tat Binds KIX.** CD spectroscopy was used to screen deletion mutants of Tat for binding to the KIX domain of CBP. The CD spectrum of Tat<sub>1–24</sub> (residues 1–24 of Tat) is reminiscent of an unfolded protein with a minimum near 200 nm (Figure 7B). Addition of Tat<sub>1–24</sub> to KIX results in a significant increase in ellipticity at the helical signature wavelengths of 208 and 222 nm over the calculated spectrum of noninteracting Tat<sub>1–24</sub> and KIX (Figure 7B). This result suggests that the N-terminus of Tat binds KIX.

The CD spectrum of ARM (residues 48–86 of Tat) is reminiscent of an unfolded protein with a minimum near 200 nm (Figure 7A). Addition of ARM to KIX results in a CD spectrum that is similar to the calculated spectra of noninteracting ARM and KIX, suggesting that ARM does not bind appreciably to KIX.

Studies of KIX binding to the regions of Tat corresponding to residues 1–48 and 21–48, both of which contain seven Cys residues, are precluded by the limited solubility of the Tat peptide fragments.

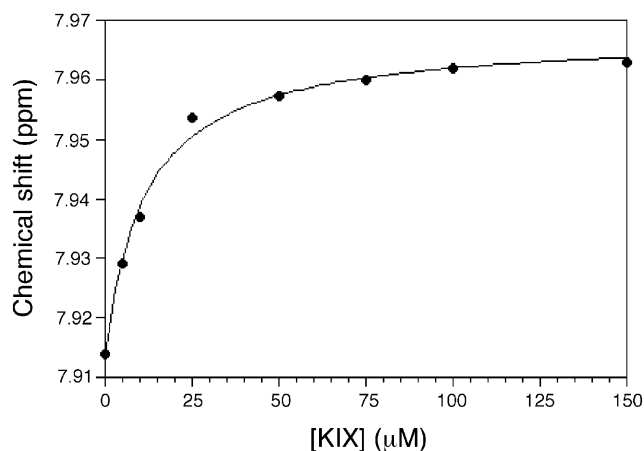


FIGURE 8: Association of KIX and Tat<sub>1–24</sub> monitored with  $^1\text{H}$  NMR spectroscopy. The change in the  $^1\text{H}$  chemical shift of His 13 C2H of Tat<sub>1–24</sub> with increasing KIX concentration is hyperbolic, as expected for a specific binding event. Fits for two independent experiments give  $K_d$  values of 10 and 12  $\mu\text{M}$ , to yield a  $K_d$  of  $11 \pm 1 \mu\text{M}$ . The error in individual chemical-shift measurements was 0.005 ppm. Experiments were performed twice with reproducible results.

Formation of the Tat<sub>1–24</sub>–KIX complex was also monitored with  $^1\text{H}$  NMR spectroscopy. Resonances of the two aromatic side chains of Tat (Trp 11 and His 13) were assigned with a TOCSY spectrum, and the changes in chemical shift measured in 1D spectra as Tat<sub>1–24</sub> was titrated with KIX. The experiment was performed in  $\text{D}_2\text{O}$  to allow exchange of the amide HN protons and thus unambiguous observation of the His and Trp side chain resonances in 1D spectra. Only the chemical shift of His 13 C2H changes appreciably upon binding KIX. The change in the His 13 C2H chemical shift upon titration with KIX is hyperbolic, as expected for a specific binding event, and yield a  $K_d$  for the Tat<sub>1–24</sub>–KIX complex of  $11 \pm 1 \mu\text{M}$  (Figure 8). This affinity is comparable to the  $K_d$  of 9.7  $\mu\text{M}$  for the complex of KIX with a 34-residue peptide derived from phosphorylated CREB (19) and 15  $\mu\text{M}$  for a 25-residue peptide derived from c-Myb (36).

## DISCUSSION

CBP and the paralog p300 bind Tat and promote transcription from the HIV-1 promoter (10, 11). Both CBP and p300 exhibit acetyltransferase activity that may be required for nucleosomal modification during the early steps of HIV-1 transcription (10, 11), and Tat recruitment of CBP may be an essential step in nucleosome modification during HIV-1 transcription (9). CBP contains several protein–protein interaction domains that bind transcription factors and regulators (Figure 1).

Using two *in vitro* assays and a dominant negative *in vivo* assay, we have localized the Tat-interacting region of CBP to the KIX domain. Since Tat binds to p300 (9), and the KIX domains of CBP and p300 share 96% sequence identity, it is likely that Tat also binds the KIX domain of p300. Furthermore, we have shown that KIX interacts with the N-terminal region of Tat from HIV-1 strain HXB2. The N-terminal 24 residues of strain HXB2 Tat share over 94% sequence identity with Tat proteins from HIV-1 strains such as LAI, pNL4-3, MN, NY-5, and SF2, suggesting that Tat proteins from different HIV-1 strains bind the KIX domain of CBP/p300.



KIX binds transcriptional activation domains via two discrete modes that employ structurally distinct surfaces. One mode is represented by the phosphorylation-induced binding of CREB (34). In contrast, MLL and c-Jun bind constitutively to a different surface of KIX than phosphorylated CREB (20, 37). Determination of the Tat binding surface of KIX awaits further structural studies of the Tat–KIX complex.

Previously, only the ARM and Cys regions (Figure 1) of Tat have been shown to be molecular recognition domains involved in transcriptional regulation. ARM binds to the RNA stem-loop transcribed within the first 60 nucleotides of the HIV-1 genome (38), and cyclin T<sub>1</sub>, a subunit of P-TEFb, interacts with the Cys-rich domain of Tat (39). Our results identify another functional region of Tat, which is involved in the recruitment of the transcriptional coactivator CBP.

Our results show that Tat is devoid of significant  $\alpha$ -helical or sheet secondary structure, in accord with a previous NMR study of 86-residue Tat (33). A number of proteins that are unfolded in isolation undergo coupled folding and binding events, including transcriptional activation domains that fold upon binding other transcription factors (40). For example, phosphorylated CREB adopts a predominantly helical structure upon binding KIX (34). The increased negative ellipticity at the helical signature wavelengths of 208 and 222 nm observed for the Tat–KIX complex (Figure 5A) suggests that helix formation occurs upon formation of the complex. Other types of induced secondary structure that make a smaller contribution to the CD spectrum may also be present in the complex, and reliable determination of the secondary structure of the complex must await further study with high-resolution methods. Since KIX is a folded, globular protein (34) and Tat is largely unfolded in isolation, it is possible that Tat undergoes a folding transition upon binding KIX. Such behavior is seen for other activation domains (40).

In conclusion, we have the defined interacting regions of Tat and CBP. Tat binds constitutively to the KIX domain of CBP, with complex formation mediated by the N-terminal region of Tat. Tat appears to fold upon binding KIX and possibly adopts a helical structure. Since Tat is a viable anti-viral drug target (14), design of peptides that inhibit Tat folding, such as HIV-1 entry inhibitors designed to inhibit gp41 folding and association (41), may present an avenue for preventing HIV propagation.

## ACKNOWLEDGMENT

We thank K. M. Campbell, H. A. Giebler, S. J. McBryant, C. D. Rithner, and K. E. Scoggin for helpful discussions, Y. Wei for purified KIX, S. J. McBryant for purified CR2, and J. K. Nyborg for plasmids. The following reagents were obtained through the NIH AIDS Research and Reference Reagent Program: GST-Tat 1(86R) from A. P. Rice; HIV-1 BH10 Tat antiserum from B. R. Cullen; pSV2tat72 from A. D. Frankel; and pBlue3'LTR-luc-A from R. E. Jeeninga and B. Berkhout.

## REFERENCES

- Jones, K. A., and Peterlin, B. M. (1994) *Annu. Rev. Biochem.* 63, 717–43.
- Frankel, A. D., and Young, J. A. (1998) *Annu. Rev. Biochem.* 67, 1–25.
- Garcia, J. A., Harrich, D., Pearson, L., Mitsuyasu, R., and Gaynor, R. B. (1988) *EMBO J.* 7, 3143–7.
- Sadaie, M. R., Rappaport, J., Benter, T., Josephs, S. F., Willis, R., and Wong-Staal, F. (1988) *Proc. Natl. Acad. Sci. U.S.A.* 85, 9224–8.
- Isel, C., and Karn, J. (1999) *J. Mol. Biol.* 290, 929–41.
- Orphanides, G., and Reinberg, D. (2002) *Cell* 108, 439–51.
- Marzio, G., and Giacca, M. (1999) *Genetica* 106, 125–30.
- Roebuck, K. A., and Saifuddin, M. (1999) *Gene Expr.* 8, 67–84.
- He, G., and Margolis, D. M. (2002) *Mol. Cell. Biol.* 22, 2965–73.
- Marzio, G., Tyagi, M., Gutierrez, M. I., and Giacca, M. (1998) *Proc. Natl. Acad. Sci. U.S.A.* 95, 13519–24.
- Benkirane, M., Chun, R. F., Xiao, H., Ogryzko, V. V., Howard, B. H., Nakatani, Y., and Jeang, K. T. (1998) *J. Biol. Chem.* 273, 24898–905.
- Chan, H. M., and La Thangue, N. B. (2001) *J. Cell Sci.* 114, 2363–73.
- Goodman, R. H., and Smolik, S. (2000) *Genes Dev.* 14, 1553–77.
- Ptak, R. G. (2002) *Expert Opin. Invest. Drugs* 11, 1099–115.
- De La Fuente, C., Santiago, F., Deng, L., Eadie, C., Zilberman, I., Kehn, K., Maddukuri, A., Baylor, S., Wu, K., Lee, C., Pumfery, A., and Kashanchi, F. (2002) *BMC Biochem.* 3, 14.
- Col, E., Gilquin, B., Caron, C., and Khochbin, S. (2002) *J. Biol. Chem.* 277, 37955–60.
- Rhim, H., Echetebe, C. O., Herrmann, C. H., and Rice, A. P. (1994) *J. Acquired Immune Defic. Syndr.* 7, 1116–21.
- Schnölzer, M., Alewood, P., Jones, A., Alewood, D., and Kent, S. B. (1992) *Int. J. Pept. Protein Res.* 40, 180–93.
- Mestas, S. P., and Lumb, K. J. (1999) *Nat. Struct. Biol.* 6, 613–4.
- Campbell, K. M., and Lumb, K. J. (2002) *Biochemistry* 41, 13956–13964.
- Van Orden, K., Giebler, H. A., Lemasson, I., Gonzales, M., and Nyborg, J. K. (1999) *J. Biol. Chem.* 274, 26321–8.
- Giebler, H. A., Loring, J. E., van Orden, K., Colgin, M. A., Garrus, J. E., Escudero, K. W., Brauweiler, A., and Nyborg, J. K. (1997) *Mol. Cell. Biol.* 17, 5156–64.
- Scoggin, K. E., Ulloa, A., and Nyborg, J. K. (2001) *Mol. Cell. Biol.* 21, 5520–30.
- Toth, F. D., Mosborg-Petersen, P., Kiss, J., Aboagye-Mathiesen, G., Hager, H., Juhl, C. B., Gergely, L., Zdravkovic, M., Aranyosi, J., Lampe, L., and Ebbesen, P. (1995) *J. Virol.* 69, 2223–32.
- Hauber, J., Perkins, A., Heimer, E. P., and Cullen, B. R. (1987) *Proc. Natl. Acad. Sci. U.S.A.* 84, 6364–8.
- Edelhoch, H. (1967) *Biochemistry* 6, 1948–54.
- Frankel, A. D., and Pabo, C. O. (1988) *Cell* 55, 1189–93.
- Klaver, B., and Berkhout, B. (1994) *J. Virol.* 68, 3830–40.
- Jeeninga, R. E., Hoogenkamp, M., Armand-Ugon, M., de Baar, M., Verhoef, K., and Berkhout, B. (2000) *J. Virol.* 74, 3740–51.
- Slice, L. W., Codner, E., Antelman, D., Holly, M., Wegrzynski, B., Wang, J., Toome, V., Hsu, M. C., and Nalin, C. M. (1992) *Biochemistry* 31, 12062–8.
- Frankel, A. D., Biancalana, S., and Hudson, D. (1989) *Proc. Natl. Acad. Sci. U.S.A.* 86, 7397–401.
- Cox, E. H., and McLendon, G. L. (2000) *Curr. Opin. Chem. Biol.* 4, 162–5.
- Bayer, P., Kraft, M., Ejchart, A., Westendorp, M., Frank, R., and Rosch, P. (1995) *J. Mol. Biol.* 247, 529–35.
- Radhakrishnan, I., Perez-Alvarado, G. C., Parker, D., Dyson, H. J., Montminy, M. R., and Wright, P. E. (1997) *Cell* 91, 741–52.
- Newton, A. L., Sharpe, B. K., Kwan, A., Mackay, J. P., and Crossley, M. (2000) *J. Biol. Chem.* 275, 15128–34.
- Zor, T., Mayr, B. M., Dyson, H. J., Montminy, M. R., and Wright, P. E. (2002) *J. Biol. Chem.* 277, 42241–8.
- Goto, N. K., Zor, T., Martinez-Yamout, M., Dyson, H. J., and Wright, P. E. (2002) *J. Biol. Chem.* 277, 43168–74.
- Huq, I., Ping, Y. H., Tamilarasu, N., and Rana, T. M. (1999) *Biochemistry* 38, 5172–7.
- Bieniasz, P. D., Grdina, T. A., Bogerd, H. P., and Cullen, B. R. (1998) *EMBO J.* 17, 7056–65.
- Wright, P. E., and Dyson, H. J. (1999) *J. Mol. Biol.* 293, 321–31.
- Root, M. J., Kay, M. S., and Kim, P. S. (2001) *Science* 291, 884–8.